Simulation of Nonlinear Circuits in the Frequency Domain

KENNETH S. KUNDERT, STUDENT MEMBER, IEEE,
AND ALBERTO SANGIOVANNI-VINCENTELLI, FELLOW, IEEE

Abstract—**Simulation in the frequency domain avoids many of the severe problems experienced when trying to use traditional time-domain simulators such as SPICE to find the steady-state behavior of analog and microwave circuits. In particular, frequency-domain simulation eliminates problems from distributed components and high-Q circuits by foregoing a nonlinear differential equation representation of the circuit in favor of a complex algebraic representation.**

This paper reviews the method of harmonic balance as a general approach to converting a set of differential equations into a nonlinear algebraic system of equations that can be solved for the periodic steady-state solution of the original differential equations. Three different techniques are applied to solve the algebraic system of equations: optimization, relaxation, and Newton's method. The implementation of the algorithm resulting from the combination of Newton's method with harmonic balance is described. Several new ways of exploiting both the structure of the formulation and the characteristics of the circuits that would typically be seen by this type of simulator are presented. These techniques dramatically reduce the time required for a simulation, and allow harmonic balance to be applied to much larger circuits than were previously attempted, making it suitable for use on monolithic microwave integrated circuits (MMIC's).

NOMENCLATURE

$\mathbb{Z}$, $\mathbb{R}$, $\mathbb{C}$	The integer, real, and complex numbers.
j	Imaginary operator, $j = \sqrt{-1}$.
t, ω	Time, radial frequency.
T_0, ω_0	Period and fundamental frequency of a periodic waveform. $T_0 = 2\pi/\omega_0$.
$P(T)$	The set of all periodic waveforms of bounded variation with period T.
$\mathfrak{F}$, $\mathfrak{F}^{-1}$	Forward and inverse Fourier operators.
x, X	Arbitrary waveform and its spectrum. $X = \mathfrak{F}x$.
$\leftrightarrow$	Laplace transform relation.
f	Function that maps waveforms to waveforms. Sometimes f is an arbitrary differentiable function, other times it is used to represent the sum of currents entering a node or nodes.
F	Function that maps spectra to spectra. Related to f in that if $y = f(x)$ then $Y = F(X)$.
H	Total number of harmonics being calculated.
N	Total number of nodes in a circuit.
k, l	Harmonic indices. $k, l \in \{0, 1, \cdots, H-1\}$.
m, n	Node indices. $m, n \in \{1, 2, \cdots, N\}$.
v, V	Node voltage waveforms, spectra.
u, U	Input current waveforms, spectra.
i, I	Function from voltage to current for nonlinear resistors and its frequency-domain equivalent.
q, Q	Function from voltage to charge for nonlinear capacitors and its frequency-domain equivalent.
y	Matrix-valued impulse response of the circuit with all nonlinear devices removed.
Υ	Laplace transform of y.
Y	Phasor equivalent to Υ.
Ω	Matrix used to multiply each particular frequency component in a vector of spectra by the right $k\omega$ to perform the frequency-domain equivalent of time differentiation ($j\Omega X = \mathfrak{F}(dx/dt)$) just as in the scalar case where ($j\omega_0 X = \mathfrak{F}(dx/dt)$).
$B_\delta(x)$	A closed ball centered at x with radius δ. $B_\delta(x) = \{y: \|x - y\| \leq \delta\}$.

Manuscript received February 15, 1986; revised May 1, 1986. This work was supported in part by the Hewlett-Packard Co., and in part by a grant from the MICRO program of the state of California.

The authors are with the Department of Electrical Engineering and Computer Sciences, University of California, Berkeley, CA 94720.

IEEE Log Number 8609726.

I. INTRODUCTION

IT IS COMMON for analog and microwave circuits to be pseudo-linear in nature. By this it is meant that input signals are sinusoidal and small enough so that few harmonics are produced. This does not imply that the nonlinearities in the circuit can be neglected. Indeed, mixers and oscillators fit this description and yet they fundamentally depend on nonlinear effects to operate. It is also common for these circuits to have a large number of distributed components such as transmission lines, whose models often include loss, dispersion, and coupling effects. These distributed components are very difficult and often impractical to simulate in the time domain because they are described using partial differential equations. While it is possible to approximate the distributed components with collections of lumped components, these approximations usually need to be of very high order to achieve sufficient accuracy, so they require a large number of lumped components. In addition, time-domain simulators are not able to exploit the pseudo-linear nature of these circuits, and often require an excessive amount of time because the steady-state solution is desired. Using a

traditional time-domain simulator to find the steady-state solution requires that the circuit be simulated until the transient solution vanishes, resulting in a very expensive simulation when the circuit is high-Q or narrow band.

Simulating these circuits in the frequency domain avoids these problems and eases the problem of formulating the equations for distributed components by transforming the time-domain differential equations into algebraic complex equations. Signals are represented using their Fourier series rather than as functions of time, so only periodic signals are representable and transients are naturally avoided. Also, the pseudo-linear nature of these circuits is naturally exploited since the amount of time required for a frequency-domain simulation is proportional to the number of frequencies present. Lastly, it is usually possible to find closed-form algebraic descriptions for distributed components in the frequency domain, so simulating these components is inexpensive.

Several other methods, all based in the time domain, have been proposed to find the steady-state solution [1]–[3]. The most popular is the shooting method. It iteratively simulates the circuit over one period intervals. On each iteration, the initial condition is varied, attempting to make the signals at the end of the period exactly match those at the beginning. The shooting method works best on forced systems that are not strongly nonlinear and have periodic solutions. They will handle autonomous circuits and forced circuits with almost-periodic solutions with some difficulty. They do not, however, handle distributed components any better than standard time-domain methods.

This paper reviews traditional approaches to finding the periodic steady-state solution for nonlinear circuits in the frequency domain and then describes several new techniques that dramatically accelerate the analysis. These techniques allow much larger circuits to be simulated. They also allow circuits to be simulated at a greater number of harmonics, which results in a substantial increase in accuracy.

After this introduction, Section I continues with a brief summary of the notations and definitions used throughout the paper. The method of harmonic balance is introduced in Section II as a way of converting a differential equation into a system of algebraic equations that can be solved for the periodic solution of the differential equation. The error mechanisms present with harmonic balance are briefly explored, and then several ways of solving the nonlinear system of equations generated by harmonic balance are studied. In particular, the harmonic programming, harmonic relaxation, and harmonic Newton methods are presented. The traditional form of harmonic relaxation is shown to be not always locally convergent, but a new modification is given and shown to provide this desirable property. A new derivation of harmonic Newton is given that does not require the presence of both positive and negative frequencies, which reduces computational complexity and memory requirements by a factor of two over previous derivations.

In Section III, several ways of increasing the efficiency of harmonic Newton are presented. The structure of the Jacobian is explored in some detail and new ways to exploit that structure are given. Finally, results are presented for several circuits, with emphasis on the time required to find the solution and the accuracy of the solution. It is shown that harmonic Newton can be both accurate and efficient.

A. Notation

When working with signals and functions, the following notation will be used: lower-case letters are used to denote time-domain variables and functions, and upper-case letters are used for frequency-domain variables and functions. Superscripts in parentheses represent iteration counts, and subscripts are used for node numbers. If the subscript is missing, then the variable is a vector representing all nodes. The argument of a waveform is time and for a spectrum it is the harmonic number. If the argument is missing, then the variable represents the whole signal (over all time or all harmonics). The superscripts R and I refer to either the real or imaginary part of the variable. A bar over a variable or function implies that it is equivalent to the unbarred version except that rather than being valid over the field of complex numbers, it is valid on $\mathbb{R}^2$. Thus

$V^{(j)} = V^{(j)}_{\cdot}(\cdot)$	the jth iteration of the voltage vector containing the complete voltage spectrum for each node;
$V_n = V_n(\cdot)$	the voltage spectrum for node n;
$V(k) = V_{\cdot}(k)$	the vector of node voltage phasors for the kth harmonic;
$V_n(k)$	the phasor for the kth harmonic of the voltage at node n;
$V_n^R(k)$, $V_n^I(k)$	the real and imaginary parts of $V_n(k)$;
$\bar{V}_n(k) = [V_n^R(k) \quad V_n^I(k)]^T$	The $\mathbb{R}^2$ equivalent of $V_n(k)$.

Similar notation is used for matrices, except the appropriate subscripts, superscripts, and arguments are doubled. For example

$J_F(V)$	the complete harmonic Jacobian of F at V;
$J_{F,mn}(V)$	the partial derivative of all harmonics of the current at node m with respect to all harmonics of the voltage at node n. $J_{F,mn}(V)$ is called a frequency conversion matrix [4];
$J_F(V, k, l)$	the partial derivative of the kth harmonic of the current at all nodes with respect to the lth harmonic of all node voltages;

$J_{F,mn}(V, k, l)$ the partial derivative of the kth harmonic of the current at node m with respect to the lth harmonic of the voltage at node n;

$\bar{J}_{\bar{F},mn}(\bar{V}, k, l)$ the $\mathbb{R}^2$ version of $J_{F,mn}(V, k, l)$;

$$\bar{J}_{\bar{F},mn}(\bar{V}, k, l) = \begin{bmatrix} J^{RR}_{F,mn}(V, k, l) & J^{RI}_{F,mn}(V, k, l) \\ J^{IR}_{F,mn}(V, k, l) & J^{II}_{F,mn}(V, k, l) \end{bmatrix}.$$

B. Definitions

Let a *signal* be a function that maps either $\mathbb{R}$ (the reals) or $\mathbb{Z}$ (the integers) into $\mathbb{R}^n$ or $\mathbb{C}^n$. The domain and range of the map are physical quantities, the domain typically being time or frequency, and the range typically being voltage or current. A signal whose domain is time is called a *waveform*, and whose domain is frequency is called a *spectrum*. All waveforms are assumed to be real valued, whereas all spectra are assumed complex valued. A waveform f is *periodic* with *period* T_0 if $f(t) = f(t + T_0)$ for all t. $P(T_0)$ denotes the set of all periodic functions of bounded variation with period T_0, i.e., $f \in P(T_0)$ implies $f: \mathbb{R} \to \mathbb{R}$ is T_0-periodic, bounded, piecewise continuous, and has at most a finite number of minima, maxima, and discontinuities per period. Functions of this type are said to satisfy the Dirichlet-Jordan criterion and can be written as a Fourier series

$$x(t) = \sum_{k=-\infty}^{\infty} X(k)\, e^{jk\omega_0 t}, \quad \text{where} \quad X(k) \in \mathbb{C},\ \omega_0 = \frac{2\pi}{T_0}$$

$$X(k) = \frac{1}{T_0} \int_0^{T_0} x(t)\, e^{-jk\omega_0 t}\, dt.$$

The kth *harmonic* of $x(t)$ is the frequency $k\omega_0$ and $X(k)$ is its *Fourier coefficient* or *phasor*. $X = \{\cdots, X(-1), X(0), X(1), \cdots\}$ is called the frequency-domain representation, or the spectrum, of x. Conversely, x is called the time-domain representation, or the waveform, of X.

A collection of devices is called a *system* if the devices are arranged to operate on an input signal (the *stimulus*) to produce and output signal (the *response*). A system is said to be in *periodic steady state* if all signals present in the system are periodic. A system is *autonomous* if both it and its stimulus are not time-varying, otherwise it is *forced*. An oscillator is an example of an autonomous system while an amplifier, a filter, and a mixer are all examples of forced systems. Lastly, an *algebraic* or *memoryless* device or system is one whose response is only a function of the present value of its stimulus, not past or future values.

II. Harmonic Balance

Harmonic balance [5], [6] (a special case of Galerkin's procedure [7], [8]) can be seen as the extension of phasor analysis [9] from linear to nonlinear differential equations. Recall that in phasor analysis the steady-state solution to an ordinary linear differential equation whose stimulus is sinusoidal is found by assuming the solution has the form $x(t) = \text{Re}\,(Xe^{j\omega_0 t})$, substituting it into the differential equation, evaluating the derivatives, and solving the resulting algebraic equation for X. When the differential equation is not linear, the solution is rarely a simple harmonic function of time but can often be approximated to first order by such a function. With harmonic balance, an approximate solution is found by assuming the solution to be purely sinusoidal and choosing its magnitude and phase to satisfy the differential equation at the fundamental only. Thus, the approximate solution $x(t) = \text{Re}\,(Xe^{j\omega_0 t})$ is substituted into the differential equation, all frequency components generated other than the fundamental are ignored, and the resulting algebraic equation is solved for X.

It was recognized that the assumed solution when using harmonic balance need not be purely sinusoidal, but rather could consist of a linear combination of sinusoids. We shall assume those sinusoids are harmonically related, making the solution periodic. If the differential equation was such that, once the solution was substituted in, the resulting equation can be factored into a sum of purely sinusoidal terms, then superposition (due to the linearity of addition) and the orthogonality of sinusoids at different harmonics can be exploited to break the resulting algebraic equation up into a collection of simpler equations, one for each harmonic. The equations are solved by finding the coefficients of the sinusoids in the assumed solution that result in the balancing of the algebraic equation at each harmonic. Hence, the name harmonic balance.

The application of harmonic balance can now be stated as a simple procedure, usually referred to as *the method of harmonic balance*.

The Method of Harmonic Balance

Given: A differential equation of the form[1]

$$f(x, \dot{x}, u) = 0 \tag{1}$$

where $u \in P(T_0)$ is the stimulus waveform, x is the unknown waveform to be found and f is continuous and real.

Step 0: Assume that the solution x exists, is real, and belongs to $P(T_0)$. Then

$$x(t) = \sum_{k=-\infty}^{\infty} X(k)\, e^{jk\omega_0 t}, \quad \text{where} \quad \omega_o = \frac{2\pi}{T_0}.$$

Step 1: Substitute the assumed solution and its derivative into f. Note that $x \in P(T_0)$ implies $\dot{x} \in P(T_0)$, and since $u \in P(T_0)$ as well, $f(x, \dot{x}, u) \in P(T_0)$. Write the resulting equation as Fourier series:

$$f(x(t), \dot{x}(t), u(t)) = \sum_{k=-\infty}^{\infty} F(X, U, k)\, e^{jk\omega_0 t} \tag{2}$$

[1]The form of the differential equation in (1) was chosen for notational convenience; harmonic balance is not limited to this form alone.

where

$$X = [\cdots, X(-1), X(0), X(1), \cdots]^T$$
$$U = [\cdots, U(-1), U(0), U(1), \cdots]^T$$
$$u(t) = \sum_{k=-\infty}^{\infty} U(k)\, e^{jk\omega_0 t}.$$

Step 2: Solve the system of nonlinear algebraic equations

$$F(X, U, k) = 0 \quad \text{for all} \quad k \in \mathbb{Z} \tag{3}$$

for X.

The statement that (3) is satisfied if and only if (1) is satisfied is called *the principle of harmonic balance*. It can easily be proved by applying Parseval's theorem to (2).

As an example of how harmonic balance can be used to find the solution to a nonlinear differential equation, consider Duffing's equation, which can be used to describe a nonlinear LC circuit

$$\ddot{x} + \lambda^2 x + \mu x^3 = A_1 \cos(\omega_0 t). \tag{4}$$

The "amount of nonlinearity" in the equation is controlled by μ, and λ is the resonant frequency of the circuit when $\mu = 0$. The steady-state solution to this equation has the form

$$x = \sum_{k=0}^{\infty} a_k \cos(k\omega_0 t),$$

where $a_k = 0$ for $k = 0, 2, 4, \cdots$.

To make the problem tractable, only a_1 and a_3 will be assumed to be nonzero. We can now substitute our assumed solution $\hat{x}(t) = a_1 \cos(\omega_0 t) + a_3 \cos(3\omega_0 t)$ into (4) as follows:

$$\tfrac{1}{4}\mu a_3^3 \cos(9\omega_0 t) + \tfrac{3}{4}\mu a_1 a_3^2 \cos(7\omega_0 t)$$
$$+ \tfrac{3}{4}\mu(a_1^2 a_3 + a_1 a_3^2) \cos(5\omega_0 t)$$
$$+ [\tfrac{1}{4}\mu(3a_3^3 + 6a_1^2 a_3 + a_1^3) + (\lambda^2 - 9\omega_0^2)a_3] \cos(3\omega_0 t)$$
$$+ [\tfrac{1}{4}\mu(3a_1^2 a_3 + 6a_1 a_3^2 + 3a_1^3) + (\lambda^2 - \omega_0^2)a_1]$$
$$\cdot \cos(\omega_0 t) = A_1 \cos(\omega_0 t). \tag{5}$$

We can now use the fact that sinusoids at different harmonics are orthogonal to rewrite (5) as a system of five equations, one for each harmonic generated by the assumed solution

$$\cos(\omega_0 t): \quad \tfrac{1}{4}\mu(3a_1^2 a_3 + 6a_1 a_3^2 + 3a_1^3) + (\lambda^2 - \omega_0^2)a_1 = A_1 \tag{6a}$$

$$\cos(3\omega_0 t): \quad \tfrac{1}{4}\mu(3a_3^3 + 6a_1^2 a_3 + a_1^3) + (\lambda^2 - 9\omega_0^2)a_3 = 0 \tag{6b}$$

$$\cos(5\omega_0 t): \quad \tfrac{3}{4}\mu(a_1^2 a_3 + a_1 a_3^2) = 0 \tag{6c}$$

$$\cos(7\omega_0 t): \quad \tfrac{3}{4}\mu a_1 a_3^2 = 0 \tag{6d}$$

$$\cos(9\omega_0 t): \quad \tfrac{1}{4}\mu a_3^3 = 0. \tag{6e}$$

Since there are only two unknowns, it is not possible to exactly satisfy all five equations. This problem results from including only a finite number of harmonics in the assumed solution when really an infinite number exist. Traditionally, the coefficients of the sinusoids in the solution are computed by solving the equations at the harmonics present in the solution. Thus, a_1 and a_3 are found by simultaneously solving (6a) and (6b). In effect, the exact solution is found for (4) with a perturbed right-hand side

$$\ddot{\hat{x}} + \lambda^2 \hat{x} + \mu \hat{x}^3 = A_1 \cos(\omega_0 t) + A_5 \cos(5\omega_0 t) + A_7 \cos(7\omega_0 t) + A_9 \cos(9\omega_0 t) \tag{7}$$

where

$$A_5 = -\tfrac{3}{4}\mu(a_1^2 a_3 + a_1 a_3^2)$$
$$A_7 = -\tfrac{3}{4}\mu a_1 a_3^2$$
$$A_9 = -\tfrac{1}{4}\mu a_3^3.$$

Notice that no mention has been made about how to solve the system of algebraic equations generated in the last step of the method of harmonic balance. Several different approaches have been used, the most notable being optimization [10]–[12], nonlinear relaxation [13], and Newton's method [14], [15]. All these methods have quite different characteristics, but all have been referred to only as harmonic balance, which has led to a certain amount of confusion. To eliminate any confusion, at least in this paper, the three approaches will be called harmonic programming, harmonic relaxation, and harmonic Newton.

A. Error Mechanisms

There are two sources of error that are of interest in harmonic balance. The first results from truncating the harmonics considered to some finite number, and the second results from not completely converging the iteration used to solve the nonlinear system of algebraic equations. If Newton's method is used, then the second source of error can be driven to an arbitrarily small level in relatively few iterations because of the method's quadratic convergence property. So this source of error will be ignored.

As shown in (7), harmonics that are not in the assumed solution end up perturbing the right-hand side of the algebraic equations. Recall that (6a) and (6b) were solved exactly for a_1 and a_3, and (6c), (6d), and (6e) were left unsatisfied; thus, (4) was also unsatisfied. Let ϵ be the amount by which (4) is not satisfied.

$$\epsilon(\hat{x}, t) = \ddot{\hat{x}} + \lambda^2\hat{x} + \mu\hat{x}^3 - A_1 \cos(\omega_0 t)$$

where

$$\hat{x}(t) = \hat{a}_1 \cos(\omega_0 t) + \hat{a}_3 \cos(3\omega_0 t).$$

From (7), it is clear that

$$\epsilon(\hat{x}, t) = A_5 \cos(5\omega_0 t) + A_7 \cos(7\omega_0 t) + A_9 \cos(9\omega_0 t).$$

Note that ϵ is orthogonal to the form of the assumed solution $\alpha_1 \cos(\omega_0 t) + \alpha_3 \cos(3\omega_0 t)$. This is a general property of harmonic balance when only a finite number of harmonics are considered.

An iterative method is used to solve the nonlinear algebraic system of equations generated by harmonic balance. Equation (6) is an example of such a system; it can be represented as

$$F(\hat{X}) = \mathbf{0}$$

where $F : \mathbb{R}^2 \to \mathbb{R}^5$ and $\hat{X} = [\hat{a}_1 \quad \hat{a}_3]^T$. In practice, this sytem is evaluated at $X = [\alpha_1 \quad \alpha_3]^T$ by computing $x(t) = \alpha_1 \cos(\omega_0 t) + \alpha_3 \cos(3\omega_0 t)$ at several time points $t_1, t_2, \cdots, t_n$, evaluating $f(t) = \ddot{x} + \lambda^2 x + \mu x^3 - A_1 \cos(\omega_0 t)$ at these time points, and converting $f(t)$ into the frequency domain using the discrete Fourier transform (DFT). In this example, $f(t)$ is band limited, so its Fourier coefficients can be calculated exactly. Only the coefficients of the first two harmonics of f are of interest; the remaining ones are discarded. However, since there are nine harmonics present, the Nyquist sampling theorem states that f must be evaluated at more than 18 time points to determine accurately the coefficients for the first two harmonics. Originally, when it was decided to compute only two harmonics, it was assumed that the coefficients at the remaining harmonics were small. So for efficiency, when calculating the Fourier series of f, the remaining harmonics are assumed to be negligible, and f is evaluated at only enough points to calculate the coefficients of the first two harmonics. Since the remaining harmonics are not zero, they will alias down onto the two, resulting in further error.

B. Circuit Analysis Using Harmonic Balance

Our goal is, given some nonautonomous, nonlinear electrical system, and some periodic stimulus, find the periodic steady-state response numerically. Note that mixers and oscillators are being specifically excluded from consideration. To simplify the presentation, the circuit equations will be formulated using nodal analysis. The node voltages are assumed to be periodic and represented as spectra with the phasors for each harmonic of each node voltage being the unknowns. When using nodal analysis, the principle of harmonic balance simply becomes a restatement of Kirchhoff's current law in the frequency domain.

Nodal analysis allows each device in the circuit to be evaluated individually, with the current resulting from each device simply added to the appropriate node. The node voltages and the sums of the currents into each node are represented in the frequency domain, which makes evaluation of the linear devices particularly easy. Phasor analysis can be used by exploiting superposition and analyzing a linear device at each frequency individually. Nonlinear devices present a problem though because it is difficult to explicitly formulate the response of a nonlinear device from a stimulus represented in the frequency domain. This problem is circumvented by transforming the stimulus of each nonlinear device into a time-domain waveform, calculating the resulting response waveform, and transforming the response back into the frequency domain. This brief excursion into the time domain will be hidden from the rest of the circuit if the response waveform is periodic, which can be assured if the nonlinear device is represented by an algebraic equation because the stimulus is periodic. If the nonlinear device is not represented by an algebraic equation (i.e., the device has memory), then the response waveform will have a transient component; thus, it will not be periodic and so cannot be accurately transformed back into the frequency domain. To prevent this, all nonlinear devices in the circuit will be assumed to be represented by algebraic equations. This restriction certainly allows resistors to be nonlinear. Surprisingly, it also allows capacitors and inductors to be nonlinear because their constitutive relations are algebraic when written in terms of the proper variables; v and q for capacitors, and i and ϕ for inductors. The conversion between i and q, and v and ϕ, must be performed in the frequency domain, where it is an algebraic operation and does not disturb the steady-state nature of the solution. Nonlinear distributed devices, such as nonlinear transmission lines, cannot be salvaged, however, so they are specifically excluded.

To show how harmonic balance would be applied to circuit analysis, consider a circuit consisting of only voltage-controlled nonlinear resistors and capacitors, linear devices of any flavor (lumped or distributed), and independent current sources whose waveforms belong to $P^N(T_0)$. Assume that the circuit has a unique periodic steady-state solution $\hat{v} \in P^N(T_0)$ that is globally asymptotically stable (i.e., $v(t) \to \hat{v}(t)$ as $t \to \infty$ regardless of $v(t_0)$) and that all device constitutive equations are differentiable when written as a function of voltage. If the circuit has N nodes, then it can be described with

$$f(v, t) = i(v(t)) + \frac{d}{dt} q(v(t)) + \int_{-\infty}^{t} y(t - \tau)\, v(\tau)\, d\tau + i_s(t) = 0 \quad (8)$$

where $t \in \mathbb{R}$ is time; v is the vector of node voltage waveforms; $i_s \in P^N(T)$ is the vector of source current waveforms; $i, q : \mathbb{R}^N \to \mathbb{R}^N$ are differentiable functions representing, respectively, the sum of the currents entering the nodes from the nonlinear conductors, and the sum of the charge entering the nodes from the nonlinear capacitors; y is the matrix-valued impulse response of the circuit

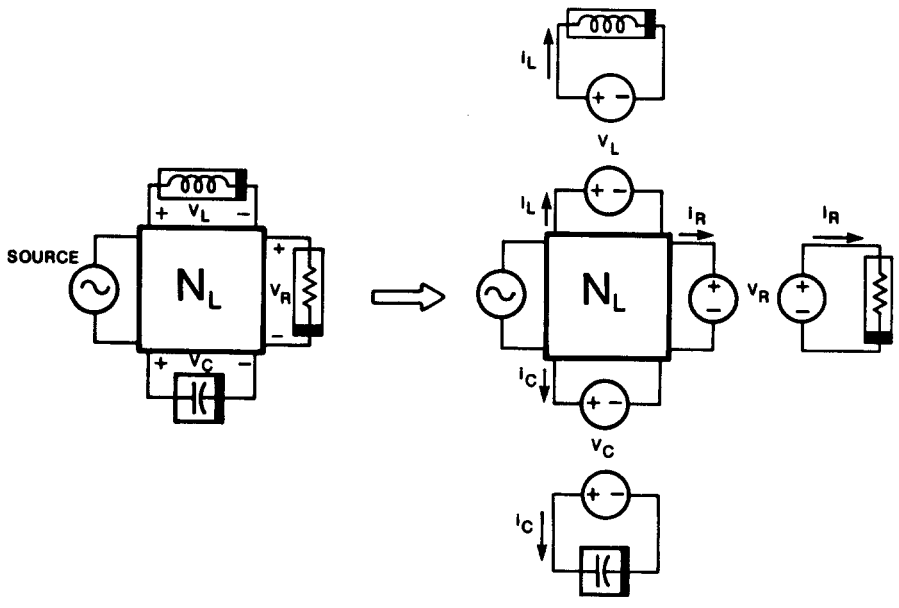

Fig. 1. Circuit interpretation of harmonic programming.

with the nonlinear devices removed;[2] and f is the function that maps the node voltage waveforms into the sum of the currents entering each node.

To use harmonic balance on (8), it is necessary to transform both $f(v)$ and v into the frequency domain. To make the problem numerically tractable, the number of harmonics considered is truncated to some finite number. The Nyquist sampling theorem indicates that this truncation is analogous to the discretization of time when integrating differential equations in the time domain and theoretically is not a limitation because, for all realizable circuits, there exists a frequency beyond which there is negligible power.

Since y is linear, the Laplace transform may be used to transform it into the frequency domain $y \leftrightarrow \Upsilon$. Furthermore, since v is periodic and the circuit is stable

$$\int_{-\infty}^{t} y(t-\tau)\, v(\tau)\, d\tau \leftrightarrow YV$$

where $V \in \mathbb{C}^{HN}$ contains the Fourier coefficients of the voltage at each node and each harmonic ($V = \mathbb{F}v$), and $Y \in \mathbb{C}^{HN \times HN}$ is a block node admittance matrix for the linear portion for the circuit

$$Y = [Y_{mn}], \qquad m, n \in \{1, 2, \cdots, N\}$$

$$Y_{mn} = [Y_{mn}(k, l)], \qquad k, l \in \{0, 1, \cdots, H-1\}$$

where m, n are the node indices; k, l are the frequency indices. Let $j = \sqrt{-1}$

$$Y_{mn}(k, l) = \begin{cases} \Upsilon_{mn}(jk\omega_0) & \text{if } k = l \\ \mathbf{0} & \text{if } k \neq l \end{cases}$$

Since v, $i(v)$, $q(v) \in P^N(T_0)$, (8) can be transformed into the frequency domain

$$F(V) = I(V) + j\Omega Q(V) + YV + I_s = \mathbf{0} \qquad (9)$$

[2]To remove a nonlinear device, simply replace its constitutive equation $y = f(x)$ with $y = 0$.

where $I_s \in \mathbb{C}^{HN}$ contains the Fourier coefficients of the source current for each node and each harmonic, $I_s = \mathfrak{F}i_s$; F, I, Q: $\mathbb{C}^{HN} \to \mathbb{C}^{HN}$, where $\mathfrak{F}f(v) = F(V)$, $\mathfrak{F}i(v) = I(V)$.

$\mathfrak{F}q(v) = Q(V)$; and $\Omega \in \mathbb{C}^{HN \times HN}$

$$\Omega = [\Omega_{mn}], \quad m, n \in \{1, 2, \cdots, N\}$$

$$\Omega_{mn} = \begin{cases} \text{diag}\,\{0, \omega_0, 2\omega_0, \cdots, (H-1)\omega_0\}, & m = n \\ \mathbf{0}, & m \neq n \end{cases}.$$

C. Harmonic Programming

It is possible to apply nonlinear programming techniques to solve (9). To do so, use $\epsilon(V) = F^*(V)\, F(V)$ as the cost function where $\epsilon(V) \in \mathbb{R}$ and the asterisk represents the conjugate transpose. An optimizer is used to find the value of V that globally minimizes $\epsilon(V)$. If a $\hat{V}$ is found such that $\epsilon(\hat{V}) = 0$, then $\hat{V}$ satisfies (9). Usually, some quasi-Newton method is used, such as the variable metric algorithm [10], [16], to achieve a superlinear rate of convergence without having to compute the Hessian of $\epsilon(V)$.

Using optimization to solve the harmonic balance equations suffers from the fact that there is a very large number of variables. If a circuit with 20 nodes is simulated at eight harmonics, then 320 variables need to be optimized. If there are many nodes in the circuit that have only linear devices attached, then it is possible to shrink the number of variables to be optimized by considering the collection of all linear devices as a single multiterminal subcircuit. The nodes with no nonlinear devices attached become internal nodes to the subcircuit and so need not be considered as optimization variables. Fig. 1 shows a convenient way of visualizing the analysis once the linear devices have been placed in a subcircuit. Here, the substitution theorem has been used to replace the nonlinear devices with sources. The resulting circuit is linear; however, the

voltage spectra for the voltage sources that are used to replace the nonlinear devices are unknown. These spectra are generated by the optimization package. Nakhla and Vlach [10] have taken this idea one step further by considering the collection of nonlinear devices as a subcircuit as well. Neither of these two approaches help when MMIC's are simulated, however, because each node in a monolithic circuit tends to have linear devices as well as nonlinear resistors and capacitors tied to them.

Using the optimizer to solve the harmonic balance equations is inefficient. To do so requires that a difficult problem, that of solving $F(V) = 0$ for V, is converted into an even harder problem, that of solving

$$\frac{dF^*(V)\, F(V)}{dV} = 0.$$

That information is lost in the conversion aggravates the situation. All information about each of the individual contributors to ϵ is lost when $F^*(V)\, F(V)$ is formed to calculate $\epsilon(V)$. It is also difficult to exploit the structure of the harmonic balance–node admittance equations, and so for these reasons, the following two approaches are preferred over harmonic programming.

D. Harmonic Relaxation

Relaxation methods are another approach that can be used to solve the algebraic set of equations that result from the application of harmonic balance. These methods are attractive when the nonlinear behavior of the circuit is very mild. Two different ways of applying relaxation methods will be presented. The first uses a form of nonlinear relaxation called *splitting* that is similar to the approach taken be Kerr [13], [17], [18]. The second combines relaxation and Newton's method; it has much better convergence properties than the first approach.

Splitting is a relaxation technique that was originally developed to solve linear systems of equations and was generalized to handle nonlinear systems [19]. As an introduction, consider the linear system

$$Ax = b \tag{10}$$

and consider the splitting of A into the sum

$$A = B - C$$

where B is nonsingular and the system $Bx = d$ is easy to solve. Then a fixed-point iteration that can be applied to find the solution of (10) is

$$x^{(j+1)} = B^{-1}(Cx^{(j)} + b)$$

where the superscript on x is the iteration count. This iteration will converge if all the eigenvalues of $B^{-1}C$ are smaller in magnitude than one.

The splitting method can be used with harmonic balance by rewriting (9) as

$$YV^{(j+1)} = -I(V^{(j)}) - \Omega Q(V^{(j)}) - I_s. \tag{11}$$

Y is assumed to be nonsingular, which implies that when all nonlinear devices are removed, there can be no floating nodes. Since linear devices are incapable of translating frequencies, the node admittance matrix for the linear portion of the circuit (Y) is block diagonal (we are assuming here that the harmonic number is the major index and the node number is the minor index). Thus, once the right-hand side of (11) has been evaluated, the task of finding $V^{(k+1)}$ can be broken into solving H decoupled linear $N \times N$ systems of equations, one for each harmonic.

To explore the convergence properties of the iteration defined by (11), the following well-known theorem [19], [20] from classical analysis is needed.

Theorem 1 (Contraction Mapping Theorem): Let C be a closed subset of $\mathbb{C}^n$. If f is a map from C into C and if there exists $\gamma < 1$ such that

$$\|f(x) - f(y)\| \leq \gamma \|x - y\|$$

for all $x, y \in C$, then f is called a contraction map on C. Furthermore, there exists a unique $\hat{x}$ (called a fixed point of f) such that $f(\hat{x}) = \hat{x}$ and given any $x^{(0)} \in C$, the sequence $\{x^{(j)}\}$ defined by $x^{(j+1)} = f(x^{(j)})$ converges to $\hat{x}$. ■

If $C = \mathbb{C}^{HN}$, then the theorem gives sufficient conditions for the global convergence of (11); however, it is difficult to apply, so a theorem giving sufficient conditions for local convergence will be presented. But first a lemma is needed.

Lemma: Suppose f maps a convex open set E contained in $\mathbb{C}^n$ into $\mathbb{C}^n$, f is differentiable in E, and there is a real number M such that $J_f(x)$, the Jacobian of f at x, satisfies

$$\|J_f(x)\| \leq M \quad \text{for every} \quad x \in E.$$

Then $\|f(x) - f(y)\| \leq M \|x - y\|$ for all $x, y \in E$. ■

The lemma is a straight-forward extension of a theorem given by Rudin [21] for $\mathbb{R}^N$.

Theorem 2: Let E be an open subset of $\mathbb{C}^n$. Suppose $f: E \to \mathbb{C}^n$ is continuously differentiable on E and can be written in the form

$$f(x) = Ax - g(x)$$

where $A \in \mathbb{C}^{n \times n}$ is nonsingular. If there exists $\hat{x} \in E$ such that $f(\hat{x}) = 0$ and if $\|A^{-1}J_g(\hat{x})\| < 1$, then there exists some $\delta > 0$ such that for all $x^{(0)}$ in the closed ball $B_\delta(\hat{x}) \subset E$ the sequence $\{x^{(j)}\}$ defined by $x^{j+1} = A^{-1}g(x^{(j)})$ converges to $\hat{x}$.

Proof: Let $\phi(x) = A^{-1}g(x)$ and choose some $\gamma \in [0, 1)$ such that $\|A^{-1}J_g(\hat{x})\| < \gamma$. Since f, and hence g, is continuously differentiable, there exists $\delta > 0$ such that for all $x \in B_\delta(\hat{x})$. $\|A^{-1}J_g(x)\| \leq \gamma$. Note that the derivative of $\phi(x)$ is $J_\phi(x) = A^{-1}J_g(x)$. From the lemma

$$\|\phi(x) - \phi(y)\| \leq \gamma \|x - y\| \tag{12}$$

for all x, y in the interior of $B_\delta(\hat{x})$, and since ϕ is continuous, (12) must hold for all of $B_\delta(\hat{x})$, not just the interior. By the contraction mapping theorem, ϕ has a unique fixed point in $B_\delta(\hat{x})$, which must be $\hat{x}$ because it is a fixed point for ϕ. Also, $\{x^{(j)}\} \to \hat{x}$ if $x^{(0)} \in B_\delta(\hat{x})$. ■

If the conclusion of Theorem 2 is applied to (11), then, to assure local convergence, we need

$$\|Y^{-1}[J_I(\hat{V}) + j\Omega J_Q(\hat{V})]\| < 1 \tag{13}$$

where $\hat{V}$ is the solution of (11). There is no reason to believe this condition will be met in practice. As an example of when it would not be met, consider a very simple circuit with only one node and analyzed at dc only. Then, $Y \in \mathbb{R}$ and $I, Q : \mathbb{R} \to \mathbb{R}$. Let $Y = 1$, $I(V) = 2V$, and $Q(V) = 0$. Then, $Y^{-1}J_I = 2$, and so the convergence criterion is not satisfied. Indeed, for this circuit, convergence will not be achieved for any $V^{(0)} \neq \hat{V}$. This example shows that relaxation using the splitting method given by (11) has poor convergence properties. In particular, even if the starting value of $V^{(0)}$ is arbitrarily close to the final solution, and regardless of how mild the nonlinearities are behaving, convergence is not assured. In fact, convergence can easily be lost if the largest conductance exhibited by any of the nonlinear devices is larger than the smallest conductance to ground present in the circuit when the nonlinear devices are removed.

The second relaxation approach to solving the algebraic harmonic balance equation (9) is to use the block Gauss-Jacobi method with a one-step Newton inner loop [19], [22] known as the block Gauss-Jacobi-Newton method. To apply this method, (9) needs to be reformulated into a system of $2H - 1$ equations; each equation calculates the vector of node currents at one frequency given the node voltages at all frequencies. (Notice we are now considering both positive and negative frequencies; this was not necessary for the splitting method.) Thus, (9) is rewritten as

$$\begin{aligned} F(V, k) &= I(V, k) + jk\omega_0 Q(V, k) \\ &\quad + Y(k, k)\, V(k) + I_s(k) = 0 \\ &\quad \text{for } k = 1 - H, \cdots, \\ &\quad -1, 0, 1, \cdots, H - 1. \end{aligned} \tag{14}$$

The block Gauss-Jacobi algorithm, when applied to (14), has the following form:

Nonlinear Block Gauss-Jacobi Algorithm

repeat
{ $j \leftarrow j + 1$;
  forall ($k \in \{1 - H, \cdots, -1, 0, 1, \cdots, H - 1\}$)
    solve $F(V^{(j)}(1 - H), \cdots, V^{(j+1)}(k), \cdots, V^{(j)}(H - 1))$ **for** $V^{(j+1)}(k)$
} **until** ($\|V^{(j+i)} - V^{(j)}\| < \epsilon$).

The equation inside the **forall** loop is solved using Newton's method for $V^{(j+1)}(k)$. Note that in this equation only $V(k)$ is a variable, and $V(l)\, l \neq k$ are constant and taken from the previous iteration. Since Newton's method (with quadratic convergence) is being performed inside an outer relaxation loop (with linear convergence), it is not necessary to fully converge the Newton iteration. In fact, it is only necessary to take one step of the "inner" Newton iteration, and doing so does not affect the asymptotic rate of convergence of the overall method [19], [22].

Block Gauss-Jacobi-Newton is similar to the splitting method, except that each equation in (14) is first linearized with one step of Newton's method rather than by just removing the nonlinearities. Applying the Gauss-Jacobi-Newton method to (14) results in

$$\frac{\partial F(V^{(j)}, k)}{\partial V(k)} [V^{(j+1)}(k) - V^{(j)}(k)] = -F(V^{(j)}, k),$$
$$k = 1 - H, \cdots, -1, 0, 1, \cdots, H - 1$$

or

$$\begin{aligned} &\frac{\partial F(V^{(j)}, k)}{\partial V(k)} V^{(j+1)}(k) \\ &\quad = \frac{\partial F(V^{(j)}, k)}{\partial V(k)} V^{(j)}(k) - F(V^{(j)}, k) \end{aligned} \tag{15}$$

where

$$\frac{\partial F(V, k)}{\partial V(k)} = \frac{\partial I(V, k)}{\partial V(k)} + jk\omega_0 \frac{\partial Q(V, k)}{\partial V(k)} + Y(k, k).$$

To simplify the calculation of this derivative, it was necessary to assume that the circuit is being analyzed at both positive and negative frequencies. Only the derivation of $\partial I(V, k)/\partial V(k)$ will be presented; the derivation of $\partial Q(V, k)/\partial V(k)$ is identical:

$$I(V, k) = \frac{1}{T_0} \int_0^{T_0} i(v(t))\, e^{-jk\omega_0 t}\, dt.$$

Now differentiate by employing the chain rule

$$\begin{aligned} \frac{\partial I(V, k)}{\partial V(k)} &= \frac{1}{T_0} \int_0^{T_0} \frac{\partial i(v(t))}{\partial V(k)} e^{-jk\omega_0 t}\, dt \\ &= \frac{1}{T_0} \int_0^{T_0} \frac{\partial i(v(t))}{\partial v(t)} \frac{\partial v(t)}{\partial V(k)} e^{-jk\omega_0 t}\, dt. \end{aligned}$$

To compute the derivative of $v(t)$, write it as a Fourier series

$$v(t) = \sum_{l=1-H}^{H-1} V(l)\, e^{jl\omega_0 t} \tag{16}$$

$$\frac{\partial v(t)}{\partial V(k)} = e^{jk\omega_0 t}.$$

Back to the derivative of $I(V, k)$

$$\frac{\partial I(V, k)}{\partial V(k)} = \frac{1}{T_0} \int_0^{T_0} \frac{\partial i(v(t))}{\partial v(t)}\, dt. \tag{17}$$

Thus, the derivative is simply the average value of the derivative waveform over one period. We used the assumption that both positive and negative frequencies were present in (16). This is necessary to avoid assuming that $V(-l) = V^*(l)$, where the asterisk represents complex conjugation. The conjugation operator is not analytic and so it is not differentiable in the complex field. This problem is surmounted in Section II-E; however, (17) is a reasonable approximation to the derivative even when only

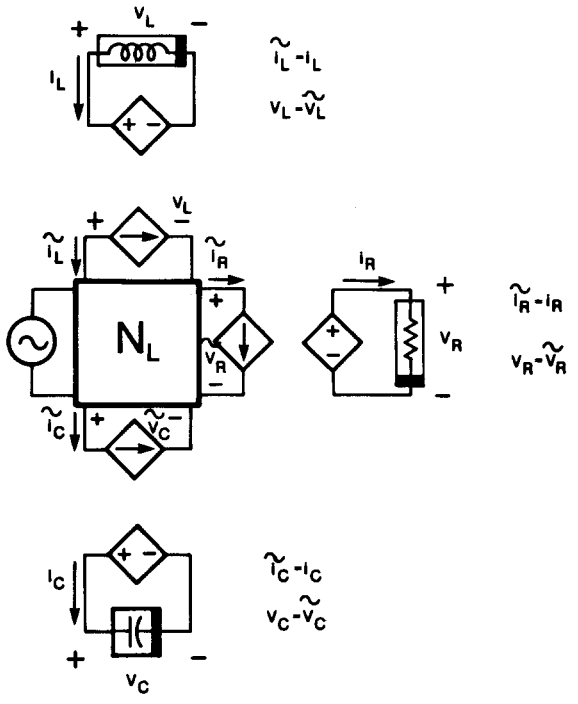

Fig. 2. Circuit interpretation of the splitting method form of harmonic relaxation.

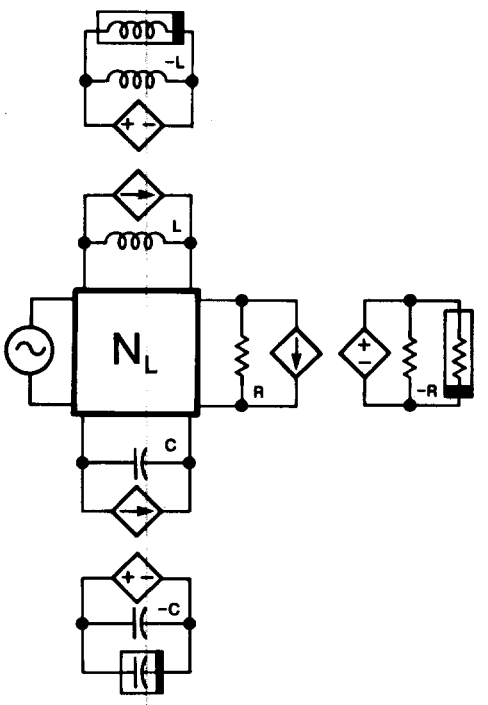

Fig. 3. Circuit interpretation of the block Gauss-Jacobi-Newton form of harmonic relaxation.

nonnegative frequencies are used. So it is probably not necessary to suffer the extra complexity of employing the negative frequencies to get the exact derivative.

The block Gauss-Jacobi-Newton iteration is well defined only if each of the equations in (14) has a unique solution at each step. In addition, convergence can be assured at least in the region local to the solution $\hat{V}$ if certain conditions are met by the Jacobian $J_F(V)$ at the solution. In particular, if F is continuously differentiable on an open set $E \subset \mathbb{C}^{HN}$ containing $\hat{V}$, and if $J_F(V) = D(V) + R(V)$, where D is a nonsingular block diagonal matrix with $D(V, k, k) = \partial F(V, k)/\partial V(k)$, then, from Theorem 2, there exists a closed ball $B_\delta(\hat{V}) \subset E$ such that for all $V^{(0)} \in B_\delta(\hat{V})$ the block Gauss-Jacobi iteration is well defined and will converge to $\hat{V}$ if $\|D^{-1}(\hat{V})\, R(\hat{V})\| < 1$. Notice that $D(V, k, k)$ is the Jacobian of the circuit at the kth harmonic. In other words, it is the node admittance matrix of the circuit at the kth harmonic where the circuit has been linearized about the solution. R represents coupling between signals at different harmonics that results from nonlinearities in the circuit. If the circuit is linear, then $R = \mathbf{0}$ and convergence is assured. The more strongly nonlinear the circuit behaves, the more coupling exists between different harmonics and the larger the terms in R become. Thus, convergence becomes less likely. So block Gauss-Jacobi-Newton is guaranteed to converge if $F(V)$ is "sufficiently linear" and if $V^{(0)}$ is sufficiently close to the solution $\hat{V}$.

To illustrate how the two relaxation methods work, consider the network shown in Fig. 2(a). In the splitting method, on each iteration, the voltages on the nonlinear devices are fixed at the values of the previous iteration, which fixes the current passed by these devices. So, in (11), the nonlinear currents are moved to the right-hand side with the constants, and, in Fig. 2, they are replaced with current sources, *a la* substitution theorem. This "linearizes" the circuit, so the node voltages can be found with Gaussian elimination. These new node voltages are then applied to the nonlinear devices, and their new current is calculated and applied to the linearized circuit, requiring it to be reevaluated on the next iteration. The linearized circuit never changes, so only forward and backward substitution is needed for reevaluation.

With block Gauss-Jacobi-Newton, the circuit is linearized by dividing the nonlinear devices into two parts. One is the best linear approximation to the nonlinear device considering the signal present on the device. The other is the nonlinear residual that when combined with the linear part gives the original nonlinear device. This division is illustrated in Fig. 3.

By viewing Figs. 2 and 3, it becomes clear why Gauss-Jacobi-Newton has better convergence properties than the splitting method: it has a better model of the nonlinear device in the linear subcircuit, so less correction is needed on each iteration. Indeed, if the nonlinear devices behave linearly, then clearly Gauss-Jacobi-Newton converges in one step while the splitting will require many, and may not even converge.

The Gauss-Jacobi-Newton method has the nice feature that it uses very little memory. The circuit is analyzed at only one frequency at a time, so space is needed for only one sparse $N \times N$ node admittance matrix; that space is reused for each frequency. This contrasts with the harmonic Newton method that will be presented next: it analyzes the circuit at all frequencies simultaneously, and so it needs a great deal more memory. The Gauss-Jacobi-Newton method is also quite fast if the circuit is behaving

linearly. However, it does have severe convergence problems when circuits behave very nonlinearly. Harmonic Newton, which can be seen as a logical extension of Gauss-Jacobi-Newton, is much more robust, but also can require much more time on near linear circuits. For this reason, techniques will be presented later that modify harmonic Newton on near linear problems to become much more like Gauss-Jacobi-Newton, resulting in a composite method that can be both fast and robust.

E. Harmonic Newton

Newton's method applied to (9) results in the following iteration:

$$V^{(j+1)} = V^{(j)} - J_F(V^{(j)})^{-1} F(V^{(j)}) \tag{18}$$

which is both locally (as is easily seen by applying Theorem 2) and superlinearly convergent. To evaluate this expression, it is necessary to compute $F(V)$ and $J_F(V)$

$$F(V) = I(V) + j\Omega Q(V) + YV + I_s$$

$$F(V) = \mathfrak{F} i(\mathfrak{F}^{-1}V) + j\Omega \mathfrak{F} q(\mathfrak{F}^{-1}V) + YV + I_s. \tag{19}$$

Thus, to evaluate the nonlinear terms in F, the node voltage spectra are transformed into the time domain, applied to the nonlinear devices, and the resulting current waveforms are converted into the frequency domain. The calculation of $J_F(V)$ is more involved, partially because $f(v)$ and v are constrained to be real functions and we desire not to use negative frequencies. Applying these two constraints results in the derivative $J_F(V)$ being unrepresentable in the complex field. To circumvent this problem, each complex number is written as an equivalent vector in $\mathbb{R}^2$. To perform this conversion, some more notation will be defined. Let $X \in \mathbb{C}$. Then define X^R, $X^I \in \mathbb{R}$, $\bar{X} \in \mathbb{R}^2$ such that $X^R = \text{Re}\ \{X\}$, $X^I = \text{Im}\ \{X\}$, and $\bar{X} = [X^R \quad X^I]^T$. Similar notation is used for vectors, functions, and matrices, Using this notation, (9) is solved with the iteration

$$\bar{V}^{(k+1)} = \bar{V}^{(k)} - \bar{J}_{\bar{F}}(\bar{V}^{(k)})^{-1} \bar{F}(\bar{V}^{(k)}) \tag{20}$$

where $\bar{F}(\bar{V})$, $\bar{V} \in \mathbb{R}^{2HN}$ and $\bar{J}_{\bar{F}} \in \mathbb{R}^{2NH \times 2NH}$ is the harmonic Jacobian, i.e.,

$$\bar{J}_{\bar{F}}(\bar{V}) = \frac{\partial \bar{F}(\bar{V})}{\partial \bar{V}} = \frac{\partial \bar{I}(\bar{V})}{\partial \bar{V}} + \bar{\Omega} \frac{\partial \bar{Q}(\bar{V})}{\partial \bar{V}} + \bar{Y}.$$

The harmonic Jacobian is organized as the block matrix

$$\bar{J}(\bar{V}) = \left[\frac{\partial \bar{F}_m(\bar{V})}{\partial \bar{V}_n}\right], \qquad m, n \in \{1, 2, \cdots, N\} \tag{21}$$

where $\bar{F}_m(\bar{V})$, $\bar{V}_n \in \mathbb{R}^{2H}$. This block matrix is referred to as the block node admittance matrix because its structure is identical to the node admittance matrix. The blocks are referred to as conversion matrices; they have the form

$$\frac{\partial \bar{F}_m(\bar{V})}{\partial \bar{V}_n} = \left[\frac{\partial \bar{F}_m(\bar{V}, k)}{\partial \bar{V}_n(l)}\right], \qquad k, l \in \{0, 1, \cdots, H-1\} \tag{22}$$

where $\bar{F}_m(\bar{V}, k) \in \mathbb{R}^2$, and

$$\bar{J}_{\bar{F},mn}(\bar{V}, k, l) = \frac{\partial \bar{F}_m(\bar{V}, k)}{\partial \bar{V}_n(l)} = \begin{bmatrix} \dfrac{\partial F_m^R(\bar{V}, k)}{\partial V_n^R(l)} & \dfrac{\partial F_m^R(\bar{V}, k)}{\partial V_n^I(l)} \\ \dfrac{\partial F_m^I(\bar{V}, k)}{\partial V_n^R(l)} & \dfrac{\partial F_m^I(\bar{V}, k)}{\partial V_n^I(l)} \end{bmatrix}.$$

This derivative consists of the sum of terms

$$\frac{\partial \bar{F}_m(\bar{V}, k)}{\partial \bar{V}_n(l)} = \frac{\partial \bar{I}_m(\bar{V}, k)}{\partial \bar{V}_n(l)} + \begin{bmatrix} 0 & -k\omega_0 \\ k\omega_0 & 0 \end{bmatrix} \cdot \frac{\partial \bar{Q}_m(\bar{V}, k)}{\partial \bar{V}_n(l)} + \bar{Y}_{mn}(k, l) \tag{23}$$

$$\bar{Y}_{mn}(k, l) = \begin{bmatrix} Y_{mn}^R(k, l) & -Y_{mn}^I(k, l) \\ Y_{mn}^I(k, l) & Y_{mn}^R(k, l) \end{bmatrix}. \tag{24}$$

Only the calculation of $\partial I_m^R(\bar{V}, k)/\partial V_n^R(l)$ will be performed; the calculation of the other terms in $\partial \bar{I}_m(\bar{V}, k)/\partial \bar{V}_n(l)$ and $\partial \bar{Q}_m(\bar{V}, k)/\partial \bar{V}_n(l)$ is similar

$$I_m(V, k) = \frac{1}{T_0} \int_0^{T_0} i_m(v(t))\, e^{-jk\omega_0 t}\, dt$$

$$I_m^R(\bar{V}, k) = \frac{1}{T_0} \int_0^{T_0} i_m(v(t)) \cos(k\omega_0 t)\, dt.$$

The function v is considered implicitly to be a function of its frequency-domain equivalent V; so the chain rule can be employed to calculate the derivative

$$\frac{\partial I_m^R(\bar{V}, k)}{\partial V_n^R(l)} = \frac{1}{T_0} \int_0^{T_0} \frac{\partial i_m(v(t))}{\partial v_n(t)} \frac{\partial v_n(t)}{\partial V_n^R(l)} \cos(k\omega_0 t)\, dt. \tag{25}$$

Now the derivative of $v_n(t)$ is calculated

$$v_n(t) = \sum_{k=-\infty}^{\infty} V_n(k)\, e^{jk\omega_0 t}$$

$$v_n(t) = V_n^R(0) + 2 \sum_{k=1}^{\infty} V_n^R(k) \cos(k\omega_0 t) - V_n^I(k) \sin(k\omega_0 t).$$

For $l \neq 0$

$$\frac{\partial v_n(t)}{\partial \bar{V}_n(l)} = \begin{bmatrix} \dfrac{\partial v_n(t)}{\partial V_n^R(l)} \\ \dfrac{\partial v_n(t)}{\partial V_n^I(l)} \end{bmatrix} = \begin{bmatrix} 2\cos(l\omega_0 t) \\ -2\sin(l\omega_0 t) \end{bmatrix}.$$

For $l = 0$

$$\frac{\partial v_n(t)}{\partial \bar{V}_n(0)} = \begin{bmatrix} 1 \\ 0 \end{bmatrix}.$$

These derivatives are now substituted into (25). So if $l \neq 0$

$$\frac{\partial I_m^R(\bar{V}, k)}{\partial V_n^R(l)} = \frac{2}{T_0} \int_0^{T_0} \frac{\partial i_m(v(t))}{\partial v_n(t)} \cos(l\omega_0 t) \cos(k\omega_0 t)\, dt$$

$$= \frac{1}{T_0}\int_0^{T_0} \frac{\partial i_m(v(t))}{\partial v_n(t)} \cdot [\cos((k+l)\omega_0 t) + \cos((k-l)\omega_0 t)]\, dt.$$

and if $l = 0$

$$\frac{\partial I_m^R(\bar{V}, k)}{\partial V_n^R(0)} = \frac{1}{T_0}\int_0^{T_0} \frac{\partial i_m(v(t))}{\partial v_n(t)} \cos(k\omega_0 t)\, dt$$

Now let $G_{mn}(k) \in \mathbb{C}$ be the kth harmonic of $\partial i_m(v(t))/\partial v_n(t)$, i.e., let

$$G_{mn}(k) = \frac{1}{T_0}\int_0^{T_0} \frac{\partial i_m(v(t))}{\partial v_n(t)} e^{jk\omega_0 t}\, dt. \tag{26}$$

Then, for $l \neq 0$

$$\frac{\partial \bar{I}_m(\bar{V}, k)}{\partial \bar{V}_n(l)} = \begin{bmatrix} G_{mn}^R(k-l) + G_{mn}^R(k+l) & G_{mn}^I(k+l) - G_{mn}^I(k-l) \\ G_{mn}^I(k-l) + G_{mn}^I(k+l) & G_{mn}^R(k-l) - G_{mn}^R(k+l) \end{bmatrix}. \tag{27}$$

and for $l = 0$

$$\frac{\partial \bar{I}_m(\bar{V}, k)}{\partial \bar{V}_n(0)} = \begin{bmatrix} G_{mn}^R(k) & 0 \\ G_{mn}^I(k) & 0 \end{bmatrix} \tag{28}$$

This completes the calculation of the harmonic Jacobian. It may now be synthesized from (21)–(28). For a one node circuit at three frequencies, the complete harmonic Jacobian would be

$$\bar{J}_{\bar{F}}(\bar{V}) = \frac{\partial \bar{I}(\bar{V})}{\partial \bar{V}} + \bar{\Omega}\frac{\partial \bar{Q}(\bar{V})}{\partial \bar{V}} + \bar{Y}$$

where

$$\frac{\partial \bar{I}(\bar{V})}{\partial \bar{V}} = \begin{bmatrix} G_{11}^R(0) & 0 & 2G_{11}^R(-1) & 2G_{11}^I(-1) & 2G_{11}^R(-2) & 2G_{11}^I(-2) \\ 0 & 0 & 0 & 0 & 0 & 0 \\ G_{11}^R(1) & 0 & G_{11}^R(0) + G_{11}^R(2) & G_{11}^I(2) & G_{11}^R(-1) + G_{11}^R(3) & -G_{11}^I(-1) + G_{11}^I(3) \\ G_{11}^I(1) & 0 & G_{11}^I(2) & G_{11}^R(0) - G_{11}^R(2) & G_{11}^I(-1) + G_{11}^I(3) & G_{11}^R(-1) - G_{11}^R(3) \\ G_{11}^R(2) & 0 & G_{11}^R(1) + G_{11}^R(3) & -G_{11}^I(1) + G_{11}^I(3) & G_{11}^R(0) + G_{11}^R(4) & G_{11}^I(4) \\ G_{11}^I(2) & 0 & G_{11}^I(1) + G_{11}^I(3) & G_{11}^R(1) - G_{11}^R(3) & G_{11}^I(4) & G_{11}^R(0) - G_{11}^R(4) \end{bmatrix}.$$

$\partial \bar{Q}(\bar{V})/\partial \bar{V}$ is similar with G replaced by C

$$\bar{Y} = \begin{bmatrix} Y_{11}^R(0) & 0 & 0 & 0 & 0 & 0 \\ 0 & 0 & 0 & 0 & 0 & 0 \\ 0 & 0 & Y_{11}^R(1) & -Y_{11}^I(1) & 0 & 0 \\ 0 & 0 & Y_{11}^I(1) & Y_{11}^R(1) & 0 & 0 \\ 0 & 0 & 0 & 0 & Y_{11}^R(2) & -Y_{11}^I(2) \\ 0 & 0 & 0 & 0 & Y_{11}^I(2) & Y_{11}^R(2) \end{bmatrix} \quad \bar{\Omega} = \begin{bmatrix} 0 & 0 & 0 & 0 & 0 & 0 \\ 0 & 0 & 0 & 0 & 0 & 0 \\ 0 & 0 & 0 & -\omega_0 & 0 & 0 \\ 0 & 0 & \omega_0 & 0 & 0 & 0 \\ 0 & 0 & 0 & 0 & 0 & -2\omega_0 \\ 0 & 0 & 0 & 0 & 2\omega_0 & 0 \end{bmatrix}.$$

Note that the second row and column of these conversion matrices consists completely of zeros, an artifact that results because phasors at dc must be real. This structural singularity in $\bar{J}_{\bar{F}}$ can be removed either by deleting the offending row and column or making the diagonal entry nonzero and always setting the dc imaginary term to zero in the right-hand vector.

By avoiding negative frequencies, the Jacobian has been converted from a complex $(2H-1)N \times (2H-1)N$ matrix to a real $2HN \times 2HN$ matrix. This conversion halves the memory required for the harmonic Jacobian and the number of operations required for its decomposition.

III. Harmonica

We are currently developing a simulator based on the harmonic Newton algorithm. Unlike previous efforts [10]–[13], [15], [17], [18] that were aimed at circuits containing only one or two nonlinear devices. *Harmonica* is designed to quickly analyze large circuits with many nonlinear devices. This advance is made possible by using harmonic Newton, by exploiting the structure and characteristics of the harmonic Jacobian, and by exploiting the linear and almost-linear behavior of the devices.

The harmonic Jacobian is organized as a block node admittance matrix. Each block is a conversion matrix that is itself a block matrix, consisting of 2×2 blocks that result from Fourier coefficients being members of $\mathbb{R}^2$ rather than $\mathbb{C}$. Conversion matrices are full if they are associated with a node that has a nonlinear device attached, otherwise they are diagonal. In a MMIC, nonlinear devices attach to most nodes, so the conversion matrices will in general be full. Since there are typically

about four nonzero elements per row and column of a node admittance matrix, and there are H rows and columns in a conversion matrix, there are typically $4H$ nonzero 2×2 blocks in each row and column of a harmonic Jacobian. Clearly, the harmonic Jacobian can be very large and much denser than typical circuit matrices. Applying traditional sparse matrix techniques [23] is not enough to solve the Newton update equation (18) efficiently. It is also necessary to reduce the density of the matrix. The Jacobian is used only to generate new iterates; it is not used when confirming convergence, so errors in the Jacobian affect only the rate and region of convergence, not the accuracy of the final solution. Approximations in the Jacobian reduce the asymptotic rate of convergence, but the gain in efficiency can more than make up for this loss.

Perhaps the easiest approximation that can be made is to simply reuse the Jacobian from a previous iteration. Clearly, if the circuit is behaving near-linearly, the Jacobian will not vary much from iteration to iteration. This idea, which is attributed to Šamanskii [19], can greatly reduce the time required for an iteration because it completely eliminates the construction and LU decomposition of the Jacobian; therefore, only the forward and backward substitution steps are needed. Some care is needed when using Šamanskii's method because if the Jacobian is varying appreciably on each step, then a bad step could be generated. On each Šamanskii step, the value of $\|F(V)\|$ should be monitored, and the step only taken if $\|F(V)\|$ is sufficiently reduced.

The second approach to approximating the Jacobian, and thus speeding the iteration, results from exploiting the natural characteristics of conversion matrices for the nonlinear devices. These matrices can be split into the sum of a Toeplitz and a Hankel matrix.[3] For example

$$\frac{\partial \bar{I}_m(\bar{V})}{\partial \bar{V}_n} = R + S$$

where

$$R = \begin{bmatrix} r_0 & r_{-1} & r_{-2} & r_{-3} \\ r_1 & r_0 & r_{-1} & r_{-2} \\ r_2 & r_1 & r_0 & r_{-1} \\ r_3 & r_2 & r_1 & r_0 \end{bmatrix} \qquad S = \begin{bmatrix} s_0 & s_1 & s_2 & s_3 \\ s_1 & s_2 & s_3 & s_4 \\ s_2 & s_3 & s_4 & s_5 \\ s_3 & s_4 & s_5 & s_6 \end{bmatrix}$$

$$r_k = \begin{bmatrix} G^R_{mn}(k) & -G^I_{mn}(k) \\ G^I_{mn}(k) & G^R_{mn}(k) \end{bmatrix} \qquad s_k = \begin{bmatrix} G^R_{mn}(k) & G^I_{mn}(k) \\ G^I_{mn}(k) & -G^R_{mn}(k) \end{bmatrix}$$

where G_{mn} is the sum of the derivative spectra for nonlinear resistors between node m and n, or from m to ground if $m = n$. This spectrum has the characteristic that the more linear the devices that generate it are behaving, the more the dc component dominates over the harmonics and the faster their magnitude drops off at higher harmonics. As a result, elements in the conversion matrix far from the diagonal will be small compared to those on the diagonal. To reduce the density of the harmonic Jacobian, these small terms far from the diagonal will be ignored.

[3]A Teoplitz matrix has the form given by $a_{ij} = r_{i-j}$ and similarly, the form of a Hankel matrix is given by $a_{ij} = s_{i+j}$.

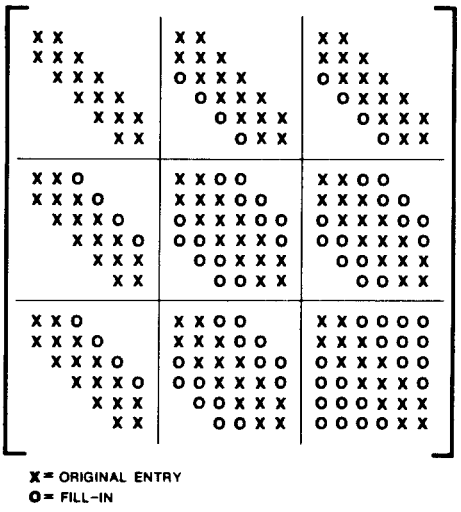

Fig. 4. Fill-in pattern of a banded block matrix.

Definition: The *guard harmonic* for a derivative spectrum is the smallest harmonic k such that

$$|G(l)| < \mu |G(0)| \qquad \text{for all} \quad l \geq k$$

where μ is a threshold parameter. Typically $\mu = 10^{-4}$.

When constructing the conversion matrices (i.e., the blocks in the harmonic Jacobian resulting from nonlinear devices), all harmonics in the derivative spectrum used to form the conversion matrix are considered negligible if they are above the guard harmonic. These harmonics are set to zero, making the conversion matrices banded about the diagonal with the bandwidth an increasing function of how nonlinear the devices contributing to the matrix are behaving. Note that if the bandwidth is restricted to one, so all entries off the main diagonal of a conversion matrix are set to zero, then harmonic Newton collapses to block Gauss-Jacobi-Newton harmonic relaxation.

Ignoring those harmonics of the derivative spectra that fall above the guard harmonics greatly increases the initial sparsity of the harmonic Jacobian; however, the Jacobian tends to fill-in during its decomposition into L and U. To see this, consider the 3×3 banded block matrix in Fig. 4. The original nonzeros are marked with crosses ($\times$) and the fill-ins are marked with circles ($\circ$). Notice the tendency of the bandwidth to increase in the blocks remaining after a major row and column have been eliminated. Also notice that, of the original nonzeros, those farthest from the diagonal of a block are due to the guard harmonics. These elements are small compared to the diagonal. The fill-ins inside the blocks always involve the guard harmonic, and so these fill-ins are assumed to be negligible. This heuristic does not have a sound theoretical basis, but is usually true if the blocks are strongly Toeplitz and both the blocks and the block matrix are strongly diagonally dominant. Thus, the nonlinearities should be resistive and behaving only mildly nonlinear,

TABLE I
COMPARISON OF TIMES FOR TWO CIRCUITS

Circuit	Conditions†	SPICE2	Harmonica		
			Harmonics		
			8	16	32
TWA	$V_{out} = 1V$	62,500‡	7	22	56
	$V_{out} = 0.5V$	*	6	16	40
μA741	$V_{out} = 1V$, $R_L = \infty$	9	6	13	29
	$V_{out} = 1V$, $R_L = 10K$	13	10	28	63
	$V_{out} = 10V$, $R_L = 10K$	14	**	365	575

†Times are given in seconds and were measured on a VAX 11/785 running UNIX 4.3BSD. *Harmonica* is written in the C programming language.
*These times were not measured, simply because little new information would be provided and the times are very expensive to measure.
**Circuit was behaving too nonlinearly for *Harmonica* to be able to converge with so few harmonics.
‡This number is an extrapolation made from measurements of times required for smaller simulation intervals. The desired time interval (two periods) caused memory usage to exceed the available 16M bytes.

and each node in the circuit should be connected to ground with an admittance that is large compared to the admittances connecting it to other nodes. These conditions are very restrictive and rarely satisfied in practice; however, the heuristic works quite well regardless and results in at least a factor of two to four speed up. The heuristic can fail though, in which case the threshold μ should be made very small and the Jacobian redecomposed. To reduce the likelihood that the heuristic will fail when nonlinear capacitors are present, the conversion matrices should be arranged so the highest harmonics and, hence, the largest admittances are placed in the upper left portion of the matrix and the smallest in the lower right.

A. Results

Execution times for the *Harmonica* are a strong function of the number of harmonics simulated, the strength of the nonlinear behavior, and the number of devices behaving nonlinearly. Before applying the techniques given in the previous section, each iteration requires $O(N^{\alpha}H^3)$ operations, where $1.1 < \alpha < 1.5$. After applying those techniques, and measuring the execution times of a few circuits, each iteration seems to require $O(N^{\alpha}H^{\beta})$ operations where $1 < \beta < 2$. The iteration count remains relatively constant as the number of harmonics changes.

The times for two circuits simulated both with *Harmonica* and SPICE [24] are presented in Table I. The first circuit is well-suited to simulation in the frequency domain and poorly suited to time-domain simulation. With the other, the roles are reversed. The first is a traveling wave amplifier (TWA) [25] that contains four bipolar transistors and ten transmission lines of noncommensurate length (Fig. 5). Note that the transmission lines are constrained to be ideal by SPICE; *Harmonica* easily handles lossy and dispersive lines. This circuit demonstrates the ease with which *Harmonica* handles circuits with distributed components.

The second circuit, a simple noninverting amplifier containing a μA 741 (Fig. 6), is troublesome to *Harmonica* because the op-amp is internally acting strongly nonlinear: the large load causing the output stage to operate class B. This example demonstrates that *Harmonica* is able to handle strongly nonlinear circuits, though it may run longer than traditional simulators. It also shows that *Harmonica* is able to handle relatively large circuits.

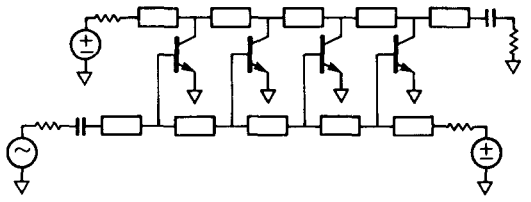

Fig. 5. The traveling-wave amplifier (TWA) schematic.

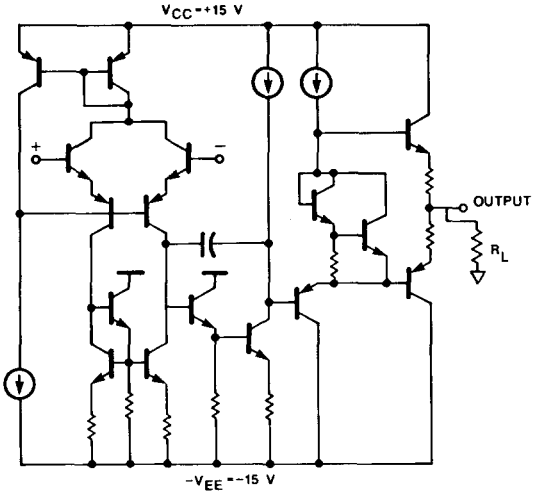

Fig. 6. Schematic of μA 741 operational amplifier. It is used in a noninverting amplifier configuration with a gain of 100.

B. Error Control

Operation in the frequency domain traditionally demands much tighter error control than is normally practiced in the time domain. The frequency-domain representation of a signal allows the resolution of small signals in the presence of large signals, with dynamic range requirements sometimes reaching 120 dB. *Harmonica* is set up to routinely achieve accuracies commensurate with these requirements.[4] There are three factors that are exploited to achieve these accuracies. First, *Harmonica* performs a true steady-state analysis with time points equally spaced over one period, so the DFT is well defined and accurate. Second, circuits typically behave near-linearly and input signals are smooth so the Fourier coefficients drop off rapidly in size at the upper harmonics. And last, the algebraic system of equations is being solved with Newton's method, which has superlinear convergence, so the system can be solved to an arbitrarily tight error tolerance within a reasonable number of iterations.

Fig. 7 shows the output spectrum of TWA when simulated using eight and 16 harmonics and the default con-

[4]Naturally, any discrepancies between the behavior of the models and the behavior of the physical devices they are modeling is desregarded.

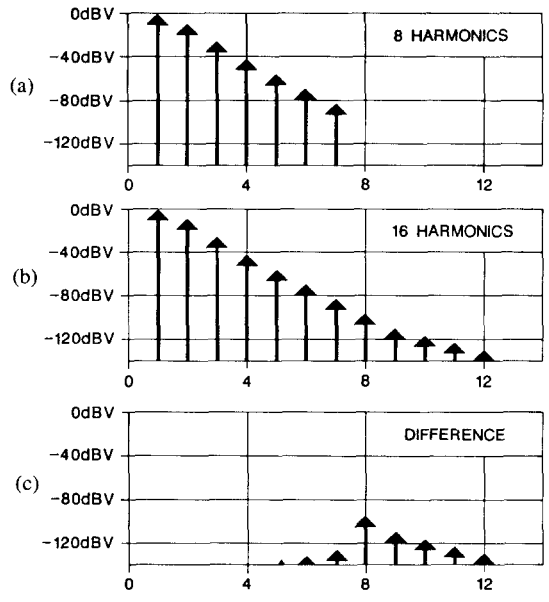

Fig. 7. Output spectra of TWA calculated by *Harmonica* using (a) eight and (b) 16 harmonics, and (c) the difference.

vergence termination criterion of 1 ppm. The difference between the outputs at eight and 16 harmonics is given in Fig. 7(c). The total error in the eight harmonic spectrum that results from not considering harmonics greater than eight amounts to about 20 ppm relative to the fundamental. The amount of error in any of the eight harmonics calculated is less than 1 ppm and is concentrated at the upper harmonics. Aliasing is responsible for most of this error, which explains why it is concentrated at the higher harmonics. The signal at the ninth harmonic is much larger than that at the 15th. The ninth aliases onto the seventh and the 15th aliases onto the first. Thus, more error is expected in the seventh harmonic than in the first.

IV. Conclusions

The harmonic balance methods, and, in particular, harmonic Newton, provide an attractive alternative to conventional time-domain simulation techniques when the periodic steady-state response of a circuit is desired. Circuits that are quite difficult to simulate in the time domain, such as high-Q circuits or circuits containing distributed components, are easily and efficiently simulated in the frequency domain. Harmonic Newton simulates circuits very accurately, providing the ability to see very small distortion products and giving the user much greater confidence in the results.

There is currently no simulator that is well matched to the task of simulating nonlinear microwave circuits, the principal reason being that all nonlinear simulators have been based in the time domain and it is difficult to simulate distributed components in the time domain. *Harmonica* is an effort to provide such a simulator to the microwave circuit design community. It is the first simulator suitable for use on large nonlinear microwave circuits.

In future work, we will try to apply harmonic Newton to both autonomous circuits and circuits that have almost-periodic solutions. We also plan to further increase the efficiency of harmonic Newton and improve its convergence properties. Lastly, we will explore applications of the harmonic Jacobian to noise analysis, sensitivity analysis, and optimization.

Acknowledgment

The authors would like to thank P. Moore for writing the parser for *Harmonica*, and W. Christopher for writing *Nutmeg*, the graphics post processor. The authors are also grateful to J. White, H. Ko, T. Quarles, and the rest of the Berkeley CAD research group, as well as J. Meyer and B. Donecker of Hewlett-Packard for many helpful discussions.

References

[1] T. J. Aprille and T. N. Trick, "Steady-state analysis of nonlinear circuits with periodic inputs," *Proc. IEEE*, vol. 60, pp. 108–114, Jan. 1972.

[2] S. Skelboe, "Computation of the periodic steady-state response of nonlinear networks by extrapolation methods," *IEEE Trans. Circuits Syst.*, vol. CAS-27, pp. 161–175, Mar. 1980.

[3] L. O. Chua and A. Ushida, "Algorithms for computing almost periodic steady-state response of nonlinear systems to multiple input frequencies," *IEEE Trans. Circuits Syst.*, vol. CAS-28, pp. 953–971, Oct. 1981.

[4] H. C. Torrey and C. A. Whitmer, *Crystal Rectifiers*. New York: McGraw-Hill, 1948.

[5] W. J. Cunningham, *Introduction to Nonlinear Analysis*. New York: McGraw-Hill, 1958.

[6] A. I. Mees, *Dynamics of Feedback Systems*. New York: Wiley, 1981.

[7] M. Urabe, "Galerkin's procedure for nonlinear periodic systems," *Arch. Ration. Mech. Anal.*, vol. 20, no. 2, pp. 120–152, Oct. 1965.

[8] J. K. Hale, *Ordinary Differential Equations*. Krieger, 1980.

[9] C. A. Desoer and E. S. Kuh, *Basic Circuit Theory*. New York: McGraw-Hill, 1969.

[10] M. S. Nakhla and J. Vlach, "A piecewise harmonic balance technique for determination of the periodic response of nonlinear systems," *IEEE Trans. Circuits Syst.*, vol. CAS-23, pp. 85–91, Feb. 1976.

[11] K. Gopal, M. S. Nakhla, K. Singhal, and J. Vlach, "Distortion analysis of transistor networks," *IEEE Trans. Circuits Syst.*, vol. CAS-25, pp. 99–106, Feb. 1978.

[12] F. Filicori, V. A. Monaco, and C. Naldi, "Simulation and design of microwave class-C amplifiers through harmonic analysis," *IEEE Trans. Microwave Theory Tech.*, vol. MTT-27, pp. 1043–1051, Dec. 1979.

[13] R. G. Hicks and P. J. Khan, "Numerical analysis of subharmonic mixers using accurate and approximate models," *IEEE Trans. Microwave Theory Tech.*, vol. MTT-30, pp. 2113–2120, Dec. 1982.

[14] S. Egami, "Nonlinear, linear analysis and computer-aided design of resistive mixers," *IEEE Trans. Microwave Theory Tech.*, vol. MTT-22, pp. 270–275, Mar. 1974.

[15] A. Ushida and L. O. Chua, "Frequency-domain analysis of nonlinear circuits driven by multi-tone signals," *IEEE Trans. Circuits Syst.*, vol. CAS-31, pp. 766–778, Sept. 1984.

[16] P. E. Gill, W. Murray, and M. H. Wright, *Practical Optimization*. New York: Academic Press, 1981.

[17] A. R. Kerr, "A technique for determining the local oscillator waveforms in a microwave mixer," *IEEE Trans. Microwave Theory Tech.*, vol. MTT-23, pp. 828–831, Oct. 1975.

[18] M. T. Faber and W. K. Gwarek, "Nonlinear–linear analysis of microwave mixer with any number of diodes," *IEEE Trans. Microwave Theory Tech.*, vol. MTT-28, pp. 1174–1181, Nov. 1980.

[19] J. M. Ortega and W. C. Rheinboldt, *Iterative Solution of Nonlinear Equations in Several Variables*. New York: Academic Press, 1970.

[20] M. Vidyasagar, *Nonlinear Systems Analysis*. Englewood Cliffs, NJ: Prentice-Hall, 1978.

[21] W. Rudin, *Principles of Mathematical Analysis*. New York: McGraw-Hill, 1976.

[22] A. R. Newton and A. L. Sangiovanni-Vincentelli, "Relaxation-based electrical simulation," *IEEE Trans. Electron Devices*, vol. ED-30, pp. 1184–1207, Sept. 1983. (Also in *SIAM Scientific and Statistical Computing*, vol. 4, no.3, Sept. 1983 and *IEEE Trans. Computer-Aided Design*, vol. CAD-3, no. 4, Oct. 1984.)

[23] K. S. Kundert, "Sparse matrix techniques," in *Circuit Analysis, Simulation and Design*, vol. 1, A. E. Ruehli, Ed. New York: North-Holland, 1986.

[24] L. W. Nagel, "SPICE2: A Computer Program to Simulate Semiconductor Circuits," Ph.D. dissertation, Univ. California at Berkeley, May 1975. Available through Electronics Research Laboratory Publications, U.C.B., 94720, Memorandum no. UCB/ERL M520.

[25] J. B. Beyer, S. N. Prasad, R. C. Becker, J. E. Nordman, and G. K. Hohenwarter, "MESFET distributed amplifier design guidelines," *IEEE Trans. Microwave Theory Tech.*, vol. MTT-32, pp. 268–275, Mar. 1984.

*

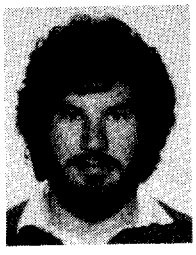

Kenneth S. Kundert (SM'86) received the M.Eng. and B.S. degrees in electrical engineering and computer sciences from the University of California, Berkeley, in 1983 and 1979, respectively. His area of specialization at the time was analog circuit design. He is currently working towards the Ph.D. degree in EECS at Berkeley and is supported by a Hewlett-Packard doctoral fellowship. His research topic is circuit simulation with particular emphasis on analog and microwave circuits.

From 1979 to 1981, he worked at Hewlett-Packard designing portions of a high performance microwave network analyzer. Since 1981, he has been at Berkeley, working first on a low-distortion switched-capacitor synchronous detector, then on a sparse matrix package for circuit simulators, and now on frequency-domain circuit simulation. His current interests include the design and simulation of analog circuits and numeric methods.

*

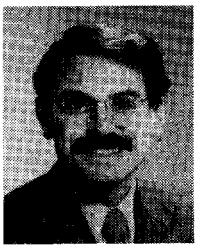

Alberto Sangiovanni-Vincentelli (M'74–SM'81–F'83) received the Dr.Eng. degree (summa cum laude) from the Politecnico di Milano, Italy, in 1971.

From 1971 to 1977, he was with the Istituto di Elettrotecnica ed Elettronica, Politecnico di Milano, Italy, where he held the position of Research Associate, Assistant and Associate Professor. In 1976, he joined the Department of Electrical Engineering and Computer Sciences of the University of California at Berkeley, where he is presently Professor and Vice-Chairman. He is a consultant in the area of computer-aided design to several industries. His research interests are in various aspects of computer-aided design of integrated circuits, with particular emphasis on VLSI simulation and optimization. He was Associate Editor of the IEEE TRANSACTIONS ON CIRCUITS AND SYSTEMS, and is Associate Editor of the IEEE TRANSACTIONS ON COMPUTER-AIDED DESIGN OF INTEGRATED CIRCUITS AND SYSTEMS and a member of the Large-Scale Systems Committee of the IEEE Circuits and Systems Society and of the Computer-Aided Network Design (CANDE) Committee. He was the Guest Editor of a special issue of the IEEE TRANSACTIONS ON CIRCUITS AND SYSTEMS on CAD for VLSI. He was Executive Vice-President of the IEEE Circuits and Systems Society in 1983. In 1981, he received the Distinguished Teaching Award of the University of California. At the 1982 IEEE-ACM Design Automation Conference, he was given a Best Paper and a Best Presentation Award. In 1983, he received the Guillemin-Cauer Award for the best paper published in the IEEE Transactions on CAS and CAD in 1981–1982. At the 1983 Design Automation Conference, he received a Best Paper Award.

Dr. Sangiovanni-Vincentelli is a member of ACM and Eta Kappa Nu.